Constraining the Hemispherical Structure in the Hidden Layer At the Top of the Earth's Inner Core

Candidate Number:

Supervisor: Prof. Keith Priestley

February 7, 2015

Abstract

Since its discovery in 1936, the Earth's inner core has been well documented by both body wave and normal mode studies. However, one area where properties are not yet well measured is the top of the inner core. The upper region of the inner core is of particular interest as it is thought that as the outer core freezes onto the inner core the variable environment at this boundary is encoded in the properties of the frozen material.

Contents

1 Introduction

The inner core was first discovered by Inge Lehmann in 1936, who used the existence of P wave arrivals within the P wave shadow zone to infer a solid-liquid boundary lying within the core mantle boundary (Lehmann (1936)). Over the following 80 years large progress has been made on measuring the properties of the inner core, but there is much still to learn.

Of particular interest is the velocity and attenuation structure, which can be used to infer the chemical and physical properties of the inner core's constituent material. Deuss (2014) gives a comprehensive review of the current state of research into this area. Current research shows that the inner core is split into two hemispheres, a western and an eastern one, each of which have differing attenuation and anisotropy properties (Waszek & Deuss (2011), Waszek & Deuss (2013)). READ PAPERS AND SUMMARISE DIFFERENCES.

The upper inner core is of particular interest, as material from the outer core is currently freezing onto it at a rate of around 1mm/year. Modelling performed by Deguen & Cardin (2009) shows that the velocity structure of the upper inner core should reflect recent processes in the lower upper core, and thus determine the WHAT history of the outer core. This in turn could give insights into areas such as how the outer core generates the Earth's magnetic field AND.

So far only large scale velocity structures have been measured, with the most recent velocity models BEING VERY COARSE GRAINED. In addition it is not clear what the limits of the methodology used here and elsewhere is to measuring the velocity structure, specifically what is the minimum depth below the inner core boundary this method can be used to resolve. In this paper we take individual earthquakes that travel to multiple seismic stations in an attempt to measure the velocity structure on the order of PUT REGION SIZE HERE. We constrain our analysis to the uppermost inner core as far as is possible, and area not yet investigated in published literature.

Section 2 gives an brief theoretical background, with section **??** describes our data collection and pre-processing. Waveform analysis is discussed in section 4 leading to regional velocity model results presented in section 5.

2 Theoretical Background

We use seismic body wave analysis in order to investigate the velocity structure of the upper inner core. These waves elastic waves, caused by earthquakes, that travel through the interior of the Earth. Below we summarise the main aspects of seismic body wave theory; for a more comprehensive review the reader is referred to Shearer (2009).

2.1 Body Wave Theory

Under the assumptions of a continuous, linearly elastic medium, infinitesimal strains and constant medium properties one can derive the elastic wave equation

$$\rho \frac{\partial^2 \vec{u}}{\partial t^2} = (\lambda + \mu) \nabla (\nabla \cdot \vec{u}) + \mu \nabla^2 \vec{u} \tag{1}$$

where u is the displacement vector, ρ the density of the medium and λ and μ Lamé parameters of the medium. A general displacement vector can be decomposed into irrotational scalar and solenoidal vector potentials such that

$$u \equiv \nabla \phi + \nabla \times \vec{\psi} \tag{2}$$

In the high frequency limit[1] equation (1) yields the Eikonal equation which describes how the rays propagate through a given velocity field.

Substituting (2) in to (1) yields two independent wave equations, one for ϕ and one for $\vec{\psi}$, which describe P-waves and S-waves respectively. P-waves are compressional with motion occurring parallel to the wave vector, whereas S-waves are transverse with motion occurring perpendicular to the wave vector.

In general we cannot make the assumption that the medium has constant parameters; this certainly is not the case for the Earth! To take varying properties into account a constant phase velocity wave equation can be generalised to have a position dependant velocity

$$\frac{\partial^2 \phi}{\partial t^2} = c^2 (\vec{x}) \nabla^2 \phi \tag{3}$$

Because the outer core is liquid with $\mu \approx 0$ and thus does not transmit S-waves, it is P-waves that are used to sample the inner core.

2.2 Sampling the Inner Core

The velocity structure of the inner core is measured using arrival times for PKIKP and PKiKP phases. Figure PUT FIGURE HERE shows the ray path for each phase; they travel almost identical paths through the Crust, Mantle and upper Outer Core, after which PKIKP reflects off the Inner Core boundary, whereas PKiKP travels just underneath the boundary in the Inner Core CHECK ME. This means that any difference in arrival times of the two phases depends only on the upper Inner Core velocity structure, which is what we seek to measure here.

All measurements are compared to the radially symmetric AK135 global velocity model (Kennett et al. (1995)), from which we seek to measure perturbations about. The residual travel time CHECK ME is defined after

[1] The high frequency ray approximation is valid for $\delta (\Delta c (\vec{x})) \ll c (\vec{x})$

Waszek & Deuss (2011) as

$$\delta t = (t_{PKiKP} - t_{PKIKP})_{model} - (t_{PKiKP} - t_{PKIKP})_{observed} \tag{4}$$

This equation can be reformulated as an integral along the ray paths

$$\delta t = \left(\int \frac{1}{v_{model}} - \frac{1}{v_{obs}} ds \right)_{PKiKP} - \left(\int \frac{1}{v_{model}} - \frac{1}{v_{obs}} ds \right)_{PKIKP} \tag{5}$$

where the path to be integrated along is indicated by the subscript outside the brackets, and in general the velocities vary as a function of position.

As the outer core has a low viscosity it is unable to support any large scale lateral heterogeneities (de Wijs et al. (1998)). We therefore expect the velocity structure of the outer core to only depend on depth, and assume that the AK135 radial symmetric model is correct for the outer core. The second integral in equation (5) then vanishes.

Taking $v_{obs} = v_{model} + \delta v$ gives

$$\delta t = \int \frac{\delta v}{v_{model}^2} ds \tag{6}$$

For depths below the Inner Core boundary of less than 50km v_{model} is constant and we assume δv is also a constant such that we are measuring only the average velocity perturbation along the ray path. We are thus left with the equation that will allow us to compute δv

$$\delta v = \frac{\delta t}{t} v_{model} \tag{7}$$

where t is the PKiKP arrival time predicted by the model.

3 Data Selection

We present regional velocity models, derived from INSERT NUMBER HERE earthquakes. The datasets are selected to meet the following criteria:

- An epicentral distance of 115° - 135° from the earthquake covers the majority of North America, where there is the highest worldwide density of seismograms.
- A hypo centre greater than 15km, to minimise possible interference between PKIKP (PKiKP) and pPKIKP (pPKiKP) waves.
- A magnitude greater than 5.3 and less than 6.3 to ensure a large enough earthquake to produce an observable signal, whilst a small enough earthquake such that the rupture mechanism is likely to be impulsive.

- A fracture mechanism that is primarily dip slip (as opposed to strike slip). As the ray paths are nearly vertical when they reach the seismic stations, we require significant amounts of energy to be focused in the vertical direction at the site of the earthquake.
- Data is selected for a 30° azimuthal range in order to only construct a small regional velocity model.

Each seismogram is filtered between 0.7Hz - 2Hz in order to focus on the expected frequency of ∼1Hz whilst removing unwanted noise. Individual seismograms are checked by hand, and only those showing a clear PKiKP signal near the predicted arrival time are kept for further analysis.

4 Waveform Analysis

The same analysis was performed on each individual event, allowing construction of a detailed velocity model for several CHANGE ME regions. Here we describe the analysis performed using the specific example of the Celebes Sea earthquake that occurred on 2014/04/16.[2]

Synthetic waveforms are computed using the WKBJ ray tracing program (Chapman (1976)), and predicted ray paths and travel times computed using the TauP toolkit (Crotwell et al. (1999)). Initial plots are shown for both real and synthetic data in figures 1 and 2 respectively, with zero time occurring at the time of the earthquake, taken from the global CMT catalogue (Dziewonski et al. (1981), Alboussière & Deguen (2012)). Overplotted are theoretical PKIKP and PKiKP travel times computed using the AK135 model (Kennett et al. (1995)). The predicted travel times agree well with the data in both cases. For shorter epicentral distances the predicted arrival time become closer, suggesting that eventually there will be a minimum distance at which the two phases will be observable. In the next subsection we attempt to quantify this minimum distance.

4.1 Quantifying minimum resolvable depth

In order to see more clearly the contributions of the individual phases to the overall seismogram we plot individual PKIKP and PKiKP synthetics, and align them to the final large upswing of the PKiKP phase. Figure 3 shows the results of this analysis. At smaller epicentral distances PKIKP gets weaker and PKiKP develops a large upswing to the left. Both of these features could mean that when measuring the peak to peak difference at low distances on the combined seismogram (or equivalently the real data) we are measuring two features of PKiKP and not one feature from each phase. This

[2]For a complete listing of all events and associated parameters see Appendix A.

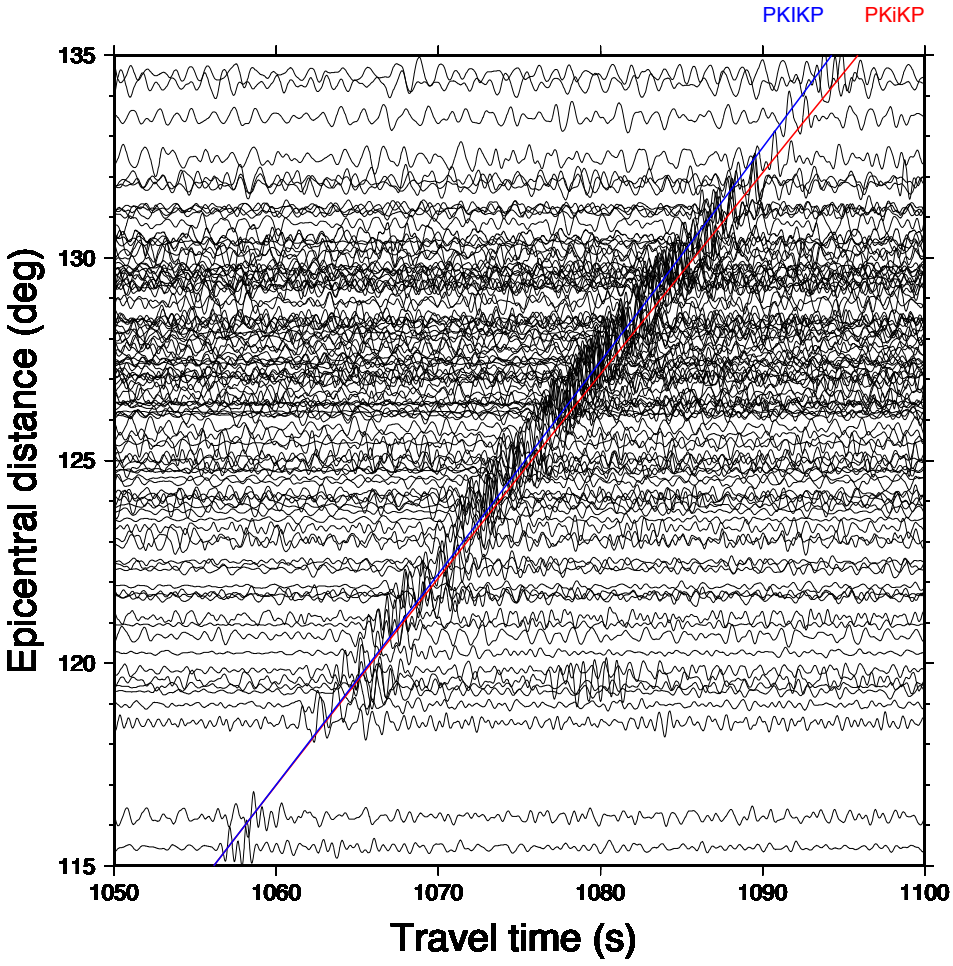

Figure 1: Real seismogram data from the Celebes Sea event after clear event selection. Each seismogram is zeroed on the earthquake time. Over plotted lines show theoretical phase arrivals computed using the AK135 model. A clear signal is seen near the expected arrival time.

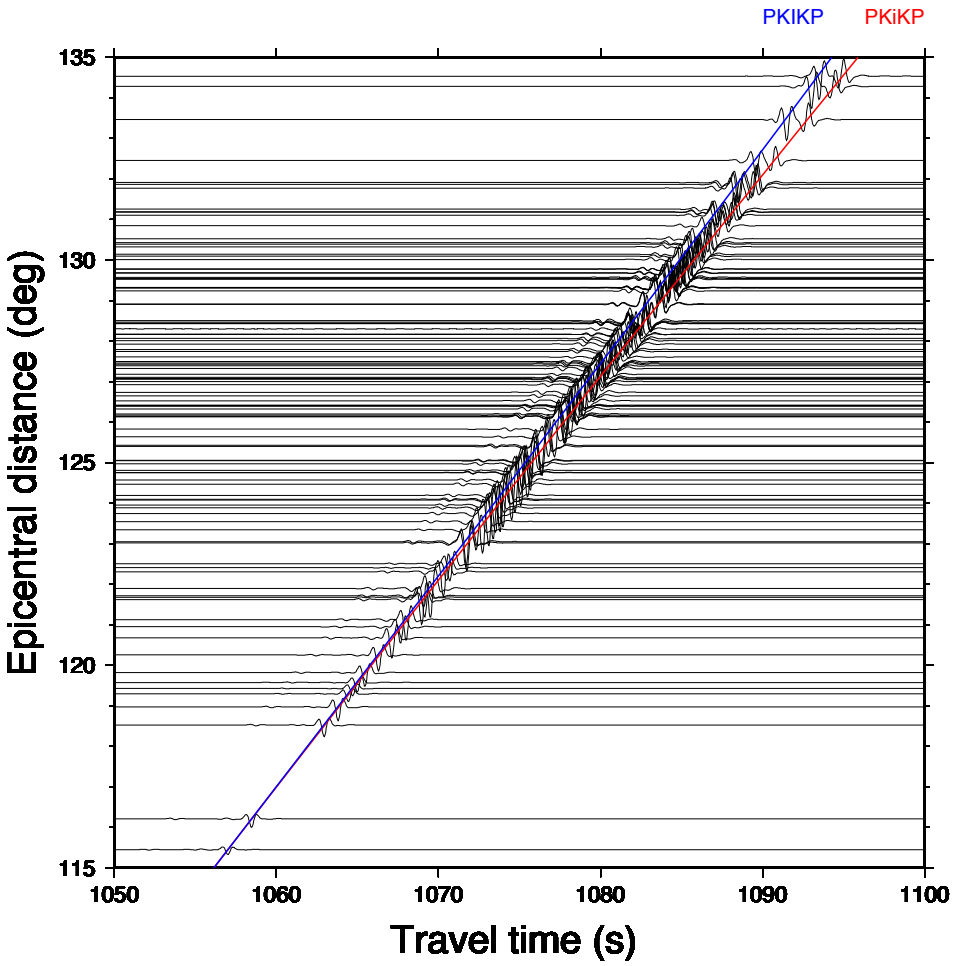

Figure 2: Synthetic seismogram data for the Celebes Sea event.. Each seismogram is zeroed on the earthquake time. Over plotted lines show theoretical phase arrivals computed using the AK135 model. The synthetic data is in broad agreement with figure 2.

criterial will be met either when PKIKP differences are larger than combined differences, or when PKiKP and combined differences coincide.

Figure 4 shows measurements of peak to peak differences for PKiKP, PKIKP and combined synthetic waveforms. It can be clearly seen that below 126° PKiKP and combined measurements coincide, thus setting 126° as the maximum epicentral distance at which the two phases can be distinguished.

5 Updated velocity models

A Event Listing

Location	Latitude	Longitude	Depth /km	Date	Time (GMT)
Celebes Sea	4.55	122.82	575.0	2014/04/16	4:28:20.0

References

Alboussière, T., & Deguen, R. 2012, Journal of Geodynamics, 61, 172

Chapman, C. H. 1976, Geophysical Research Letters, 3, 153

Crotwell, H. P., Owens, T. J., & Ritsema, J. 1999, Seismological Research Letters, 70, 154

de Wijs, G. A., Kresse, G., Vocadlo, L., et al. 1998, Nature, 392, 805

Deguen, R., & Cardin, P. 2009, Nature Geoscience, 2, 419

Deuss, A. 2014, Annual Review of Earth and Planetary Sciences, 42, 103

Dziewonski, A. M., Chou, T.-A., & Woodhouse, J. H. 1981, Journal of Geophysical Research, 86, 2825

Kennett, B. L. N., Engdahl, E. R., & Buland, R. 1995, Geophysical Journal International, 122, 108

Lehmann, I. 1936, Publications du Bureau Central Séismologique International, 14, 87

Shearer, P. M. 2009, Introduction to Seismology, 2nd edn. (Cambridge University Press)

Waszek, L., & Deuss, A. 2011, Journal of Geophysical Research, 116, B12313

—. 2013, Geophysical Journal International, 195, 2005

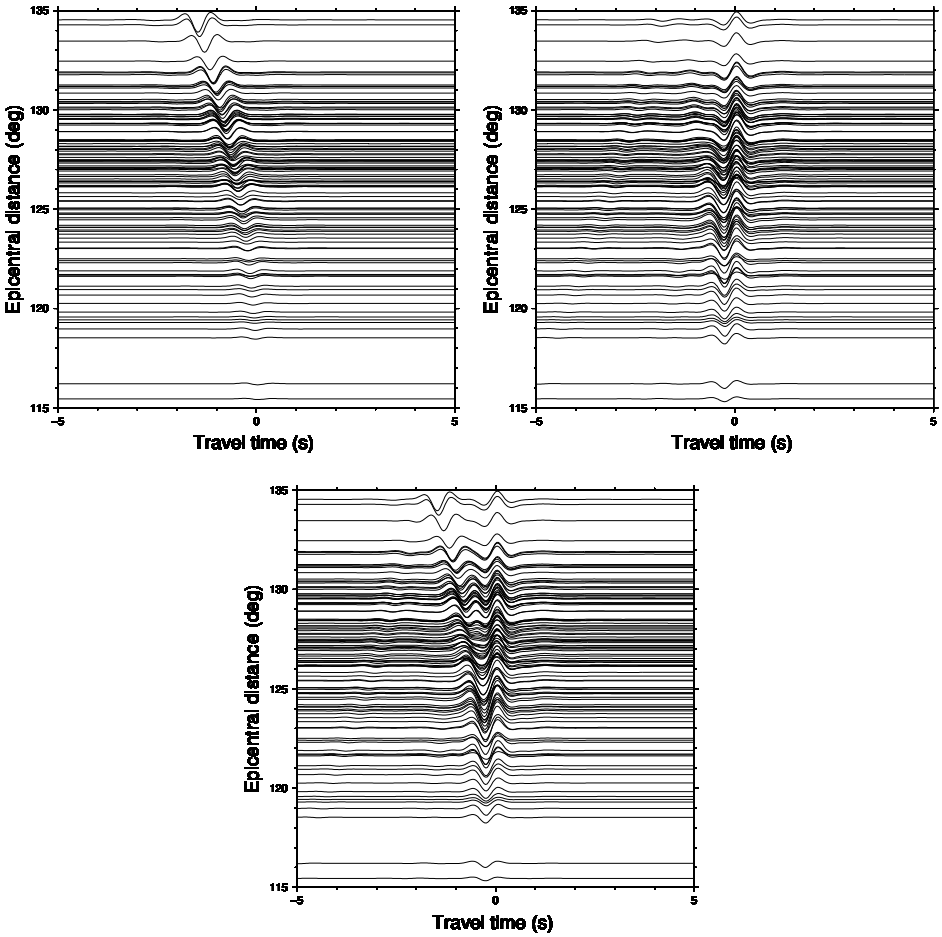

Figure 3: Separated PKIKP (top left) PKiKP (top right), and combined (bottom) synthetic seismograms for the Celebes Sea event. At distances below $\sim 125^\circ$ the combined waveform is dominated by the PKiKP waveform, and thus it is impossible to detect the arrival of PKIKP.

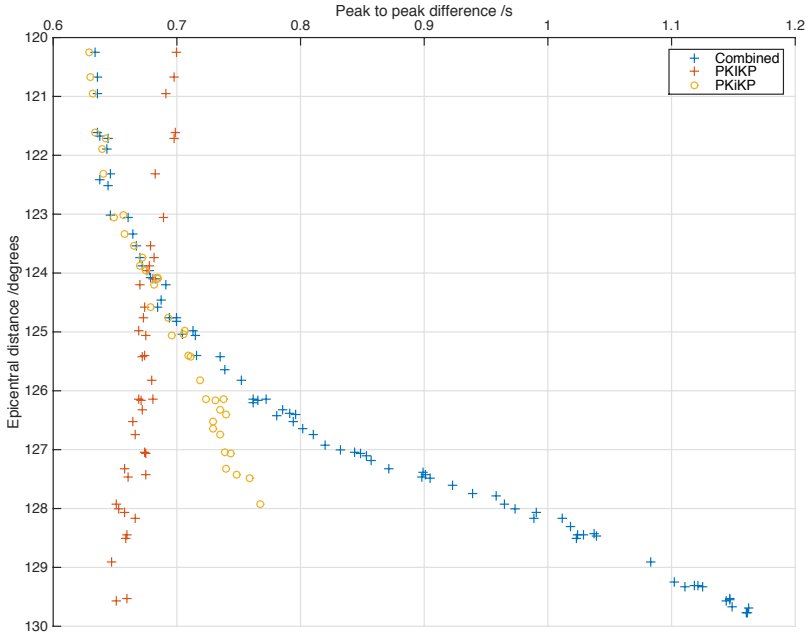

Figure 4: Peak to peak travel times recorded from synthetic data generated for the Celebes Sea earthquake. PKIKP measurements cross combined measurements at 124°, and PKiKP measurements coincide with combined measurements below 126°. The larger of these two sets a minimum distance at which we can make reliable PKiKP - PKIKP residual travel time measurements.